Title: Interfacial Characterization of SLM Parts in Multi-material Processing: Intermetallic Phase Formation between AlSi10Mg and C18400 Copper Alloy

Authors:

S.L. Sing (Swee Leong Sing)

L.P. Lam (Lit Ping Lam)

D.Q. Zhang (Dan Qing Zhang)

Z.H. Liu (Zhong Hong Liu)

C.K. Chua (Chee Kai Chua) mckchua@ntu.edu.sg +65 6790 5486 *corresponding author

Affiliations:

Singapore Centre for 3D Printing, School of Mechanical & Aerospace Engineering, Nanyang Technological University

Address: HW1-01-05, 2A Nanyang Link, Singapore 637372

Keywords: Additive manufacturing, 3D printing, Rapid prototyping, Multi-material, Selective laser melting

Abstract:

Multi-material processing in selective laser melting (SLM) using AlSi10Mg and UNS C18400 copper alloy was carried out. The interfacial characteristics were analyzed with FIB, SEM, XRD, EDS and EBSD techniques. Al_2Cu intermetallic compound was formed at the Al/Cu bond interface after the SLM process. The tensile strength of Al/Cu SLM parts was evaluated to be 176 ± 31 MPa and flexural strength under a 3 point bending test was evaluated to be around 200 MPa for Cu at root and 500 MPa for Al at root. Further analysis suggested that the formation of intermetallic compounds translated the fracture mechanism at the interface from ductile to brittle cleavage. The microhardness values also varied along the interface with high microhardness at the interface due to the intermetallic compounds.

1. Introduction

Selective laser melting (SLM) is an additive manufacturing (AM) technique that fabricates net shape parts from the melting and fusion of powder material in a layer by layer fashion [1, 2]. SLM has proven to produce high density, near net-shape parts with good mechanical properties. It also has the ability to produce parts with design configurations conventional manufacturing process cannot produce. In most cases however, the SLM process handles only one material type at a time. While producing functionally graded material (FGM) can be easily achieved in SLM by varying the porosity, fabricating parts with functionally graded properties using multi-material processing in SLM is possible but difficult to achieve [3].

Various studies have been carried out in recent years on multi-material additive manufacturing methods and has been summarised previously [4-6]. However, for powder bed fusion technologies such as SLM and electron beam melting (EBM), limited research has been carried out. The multi-material processing between Ti6Al4V and copper has been carried out in EBM using discretized steps [5]. The mechanical properties and microstructures obtained at discrete material regions are different compared to the same materials processed separately by EBM in single run. In particular, for SLM, fundamental bonding characteristics between copper and H13 has been studied, using a modified CNC machine with purpose-built rig, Nd:YAG laser power source and a nozzle powder dispensing system [7]. A noticeable amount of diffusion was obtained between copper and H13 and good bonding was achieved. In another study, the bonding characteristics and mechanical properties between multi-materials metallic parts formed using copper alloy UNS C18400 and 316L stainless steel fabricated by SLM were investigated [4]. Good metallurgical bonding was also obtained between these two materials; however, the interface exhibited tensile strength higher than that of copper and lesser than that of stainless steel.

The objective of this study is to study the interfacial characteristics of bimetallic materials formed by SLM using AlSi10Mg and UNS C18400. The fabrication is achieved using a novel approach of separating the dispensing system into two compartments so that different materials can be deposited in each of the two coating direction. The study also explores the formation of intermetallic between these two materials during the SLM process.

2. Experiment

2.1 Material and Applications

Two different representative materials, UNS C18400 copper alloy (with a D_{99} = 38 µm particle size distribution) and AlSi10Mg (20 µm to 63 µm normally distributed), were used in this study on SLM of multi-material. Aluminium and copper alloys were specially chosen because Al and Cu composites combine the benefits of high conductivity of copper together with the light weight and lower cost of aluminium [8] with Al/Cu clads being 50 % lighter than copper with similar conductivity while being 30 - 40 % cheaper [9]. Aluminium and copper composites are widely used for armoured cables and television yoke coils [9]. Joints between aluminium and copper are also often required in electrical components [10] and solar collectors [11] due to high specific conductivity and good corrosion resistance. It is also used as a transition piece in high direct-current bus systems where previously aluminium and copper were bolted together. These joints however were electrically unstable in the long term and often failed due to galvanic corrosion. By welding the joints together, the interior could be sealed from atmospheric contaminants and the joint resistance could be stabilized [12].

2.2 Equipment and Process

The SLM equipment used in this work is the SLM250 HL from SLM Solutions AG. The hopper powder feeding mechanism allows the integration of a specially designed separator in the recoater where two or more materials can be stored and deposited selectively in each layer. Some modifications to the recoating software as well as CAD file were carried out where the process parameters can be defined separately. The SLM machine is equipped with a Gaussian beam fiber laser of power up to 400 W with a focal diameter of 80 µm. The process parameters for each material and their resultant relative densities are shown in Table 1. The process parameters used were first optimized on the individual materials. These parameters were then applied on the multi-material processing. The density measurements were measured using Archimedes' Principle using XSE204 Analytical Balance from Mettler-Toledo.

Table 1. Process parameters and resultant relative density

	UNS C18400 Copper	**AlSi10Mg**
Laser power (W)	300	350
Laser scan speed (mm/s)	400	1140
Layer thickness (µm)	50	50
Hatch spacing (mm)	0.15	0.17
Remelting	Yes	No
Relative density (%)	92.9	98.1

Fig. 1 shows a simple Al/Cu electrical connector produced using the process parameters in Table 1. A tensile specimen produced after wire-cutting from a block fabricated using the same process parameters is also shown in the same figure.

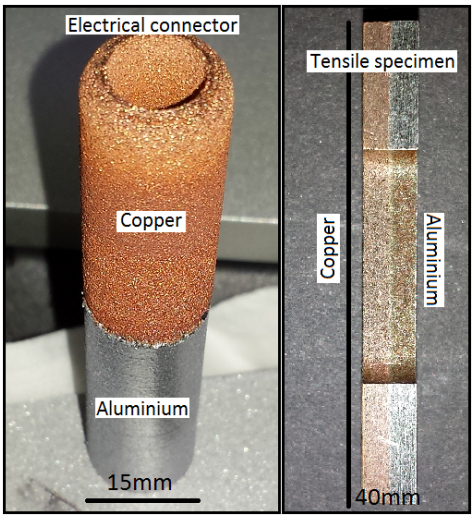

Fig.1. Aluminum/Copper electrical connector and tensile specimen

2.3 Interfacial Characterization

The SLM samples were ion milled to characterize the aluminum/copper interface using different techniques, namely, focused ion beam imaging (FIB) from FEI Helious 600i, field emission scanning electron microscopy (FESEM) JSM7600 from JEOL, electron dispersive spectroscopy (EDS) from Oxford Instruments X max, electron back scattered diffraction (EBSD) from Oxford Instruments Nordlys and X-ray Diffraction (XRD) from Empyrean, PANalytical.

2.4 Mechanical Characterization

Small tensile coupons with gauge length of 15 mm were produced using wire-cut electrical discharge machining (EDM) from blocks fabricated by SLM for individual materials, i.e. AlSi10Mg, UNS C18400 and the bimetallic aluminum/copper (Al/Cu) laminates. An Instron

Static Tester 5569, 50 kN machine was used and a strain rate of 1mm/min was applied to all three materials systems. The microhardness of the aluminum/copper samples was measured using Vickers hardness test where a load of 100 g and a loading time of 15 s were used. Bending tests were carried out, based on ASTM E290, to characterize the bonding strength between AlSi10Mg and C18400.

3. Interfacial Characteristics

3.1 Focused Ion Beam and Scanning Electron Microscopy Imaging

FIB imaging was used to observe the Al/Cu bonding interface as well as microstructure of copper formed by SLM. This technique was chosen due to the advantage of high grain contrast obtained when imaging with ions. FESEM was used to study the microstructural morphology of AlSi10Mg alloy and the interfacial morphology. Clear distinct copper rich and aluminum rich regions can be identified as shown in Fig. 2.

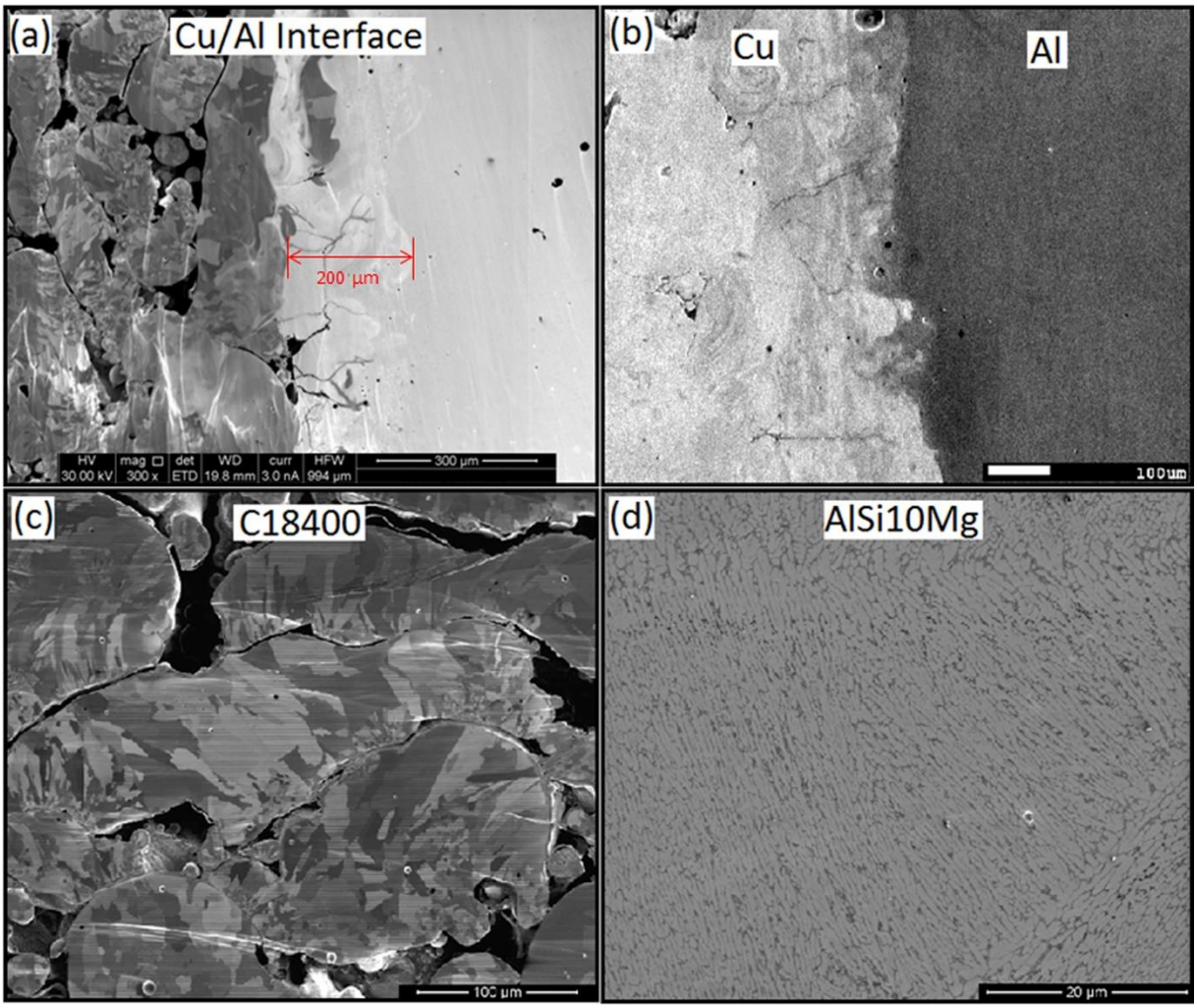

Fig. 2. (a) FIB image of Cu/Al interface; (b) SEM image of Cu/Al interface; (c) FIB image of copper; (d) SEM image of AlSi10Mg

An intermixed region can be found at the interface due to the movement of elements assisted by diffusion. The intermixed region is estimated to be 200 µm. This indicates significant dilution between AlSi10Mg and copper alloy, approximately across 4 layers of powder depositions, which is indicative of good metallurgical bonding. When a layer of copper powder is melted over the solidified aluminum surface, the top surface of aluminum gets remelted due to the penetration depth of the laser. The remelted aluminum and melted copper form a common melt pool consisting of mixture of aluminum and copper. Therefore, in the first layer of copper melt, there will be the highest proportion of aluminum. This phenomenon is repeated in the

subsequent layers until the penetration depth of the laser is lower than the layer of copper powder deposited. At this critical layer thickness, the percentage of aluminum undergoing remelting is zero, and copper powder alone undergoes melting and rapid solidification. This creates the dilution effect, commonly seen in cladding [4].

Cracks can be seen along some segments of the interface as shown in Fig. 2(a). Laser interacts differently with copper and aluminum and due to the difference in thermal coefficients between the two materials resulting in uneven expansion and contraction during the rapid solidification in SLM, cracks can be formed. Intermetallic compounds formation can also lead to brittleness and cracking of the interface [8]. In the bulk AlSi10Mg, it is almost free from porosity or any other defects but significant amount of porosity was observed on the copper side because of inadequate melting due to the high reflectivity and thermal conductivity of copper [13]. These accounted for the dense structure of the AlSi10Mg and the porous structure of copper. The density of copper can be improved by working with the variable parameters of SLM, such as lowering the layer thickness, increasing the preheating temperature, reducing scan speed, increasing laser power or reducing the hatch spacing. By doing so, the energy density applied to the material will be higher which will then compensate for the loss due to reflection and conduction.

A mixture of microstructures is shown in the intermixed region, as shown in Fig. 3. Independent and highly refined microstructures of AlSi10Mg and copper alloy can be clearly seen in the intermixed region. This finer grain structure can be attributed to the high cooling rates in SLM [14]. However, in the unmixed aluminium and copper regions, the grains are not as small compared to the intermixed region. This is expected as grains growth occurs in the unmixed regions due to the multiple thermal excursions during the SLM process, layer by layer, resulting in grains extending over multiple layers.

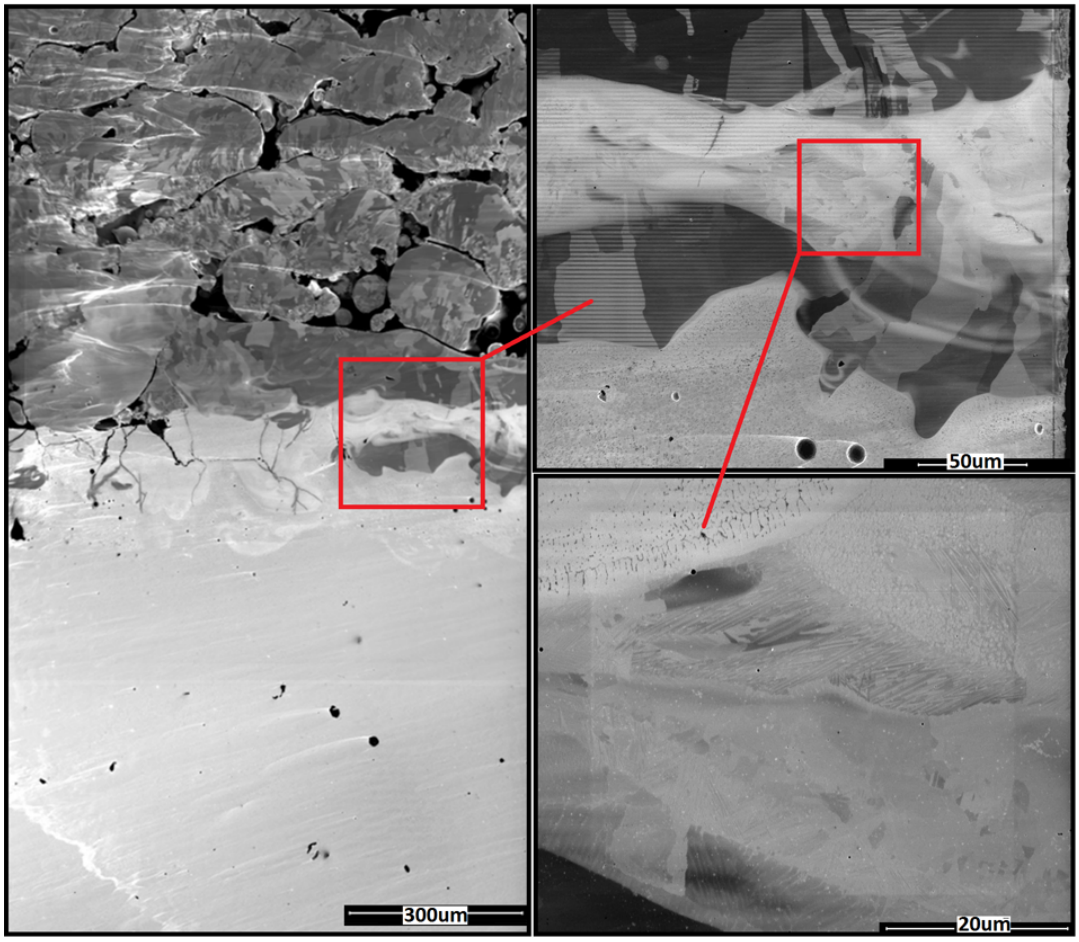

Fig. 3. Close up of the Cu/Al interface showing intermetallic morphology

3.2 Energy Dispersive Spectroscopy

EDS mapping was carried out at 3 areas in order to identify the extent of diffusion between AlSi10Mg and copper at the intermixed region. The 3 areas are

- Area 1 – interface near the bulk copper
- Area 2 – middle of interface of aluminum/copper
- Area 3 – interface near the bulk AlSi10Mg

The elemental mapping showed distinctive mixtures of Al, Si and Cu at all 3 regions as shown in Fig. 4.

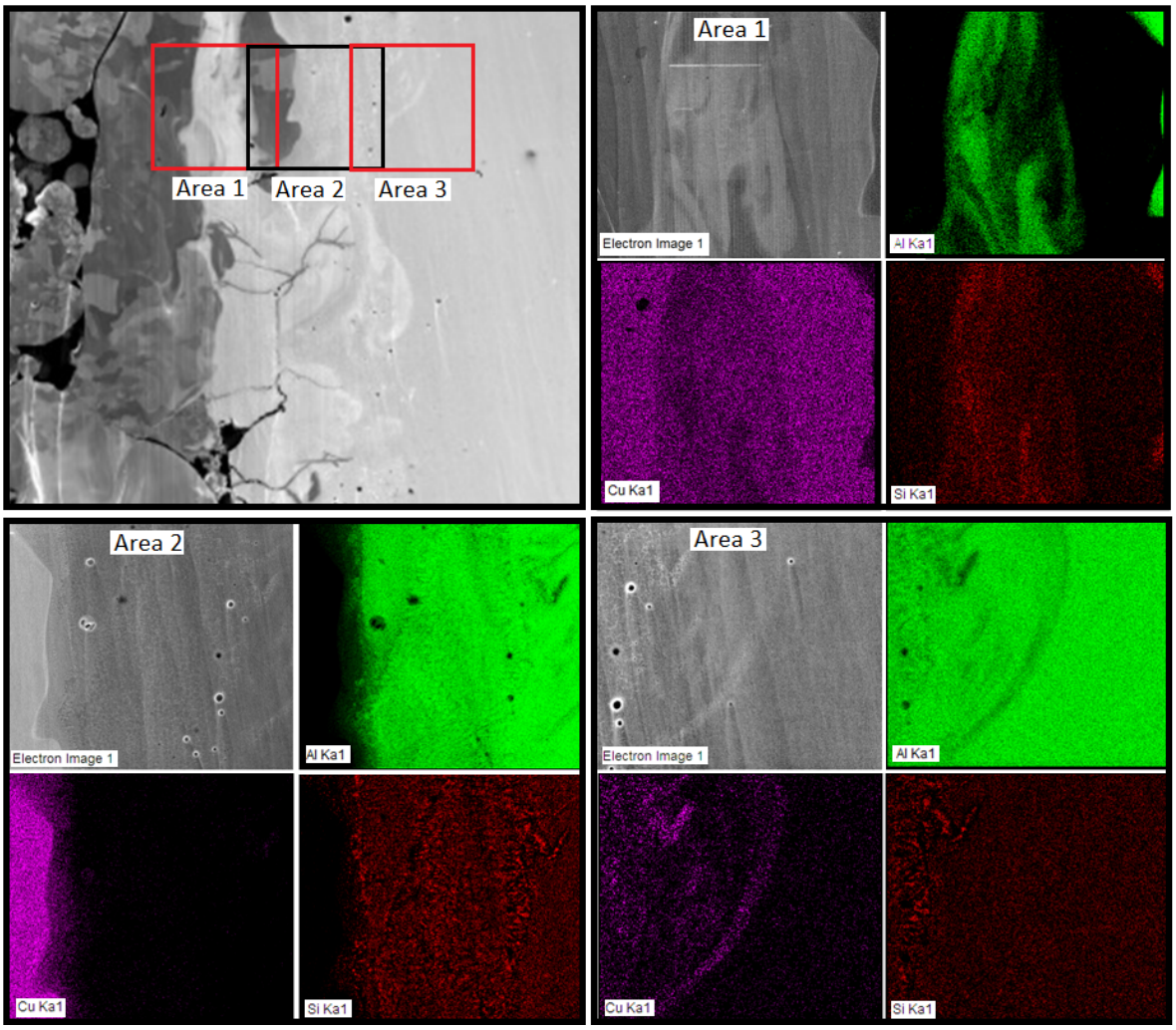

Fig. 4. EDS mapping of aluminum/copper interface at near bulk copper (Area 1), interface (Area 2) and near bulk AlSi10Mg (Area 3)

The EDS results also showed the diffusion of Al, Si and Cu to either side of the interface, as indicated by the difference in mapping across the 3 areas. In Area 1, the majority of the specimen is made up of rich Cu regions with even distribution of Si. However, the flow of Al is limited to specific region the area. This may be due to the impeded flow of the melted material during the SLM process, resulting in Al concentration in specific regions rather than continuous flow. In Area 2, the copper and aluminum are observed to be segregated to specific regions in the area. The flow of Al and Cu may be impeded due to the similarity of atomic size of Al (125 pm), Si (117.6 pm) and Cu (128 pm) and the atomic weight of Al and Si being

significantly lower than that of Cu, resulting in segregation of Cu due to their restricted movement during the SLM process. Furthermore, the formation of intermetallic may affect the diffusion rates of the elements [15]. In Area 3, the majority of the specimen is made up of Al rich regions with even distribution of Si. This is due to the usage of pre-alloyed AlSi10Mg powder for SLM. It can be observed that there is diffusion of Cu into the Al rich regions, indicating good diffusion of the elements. Literature data for diffusion of copper and aluminum also confirm a higher diffusion rate of copper in aluminum [8]. This may be aided by the heavier Cu powder particles sinking into the bottom of the melt pools during the SLM process, resulting in more even distribution of the elements in this area. As the absorptivity of copper is lower than aluminium, melting took place more in the aluminium side.

3.3 Electron Backscatter Diffraction

EBSD was carried out to capture the grain size distribution at the copper, AlSi10Mg and Cu/Al interface. The color coded inverse pole figure, where points on the sample with a <111> axis parallel to the surface normal are blue, <101> green and <001> red and intermediate orientations have intermediate colors.

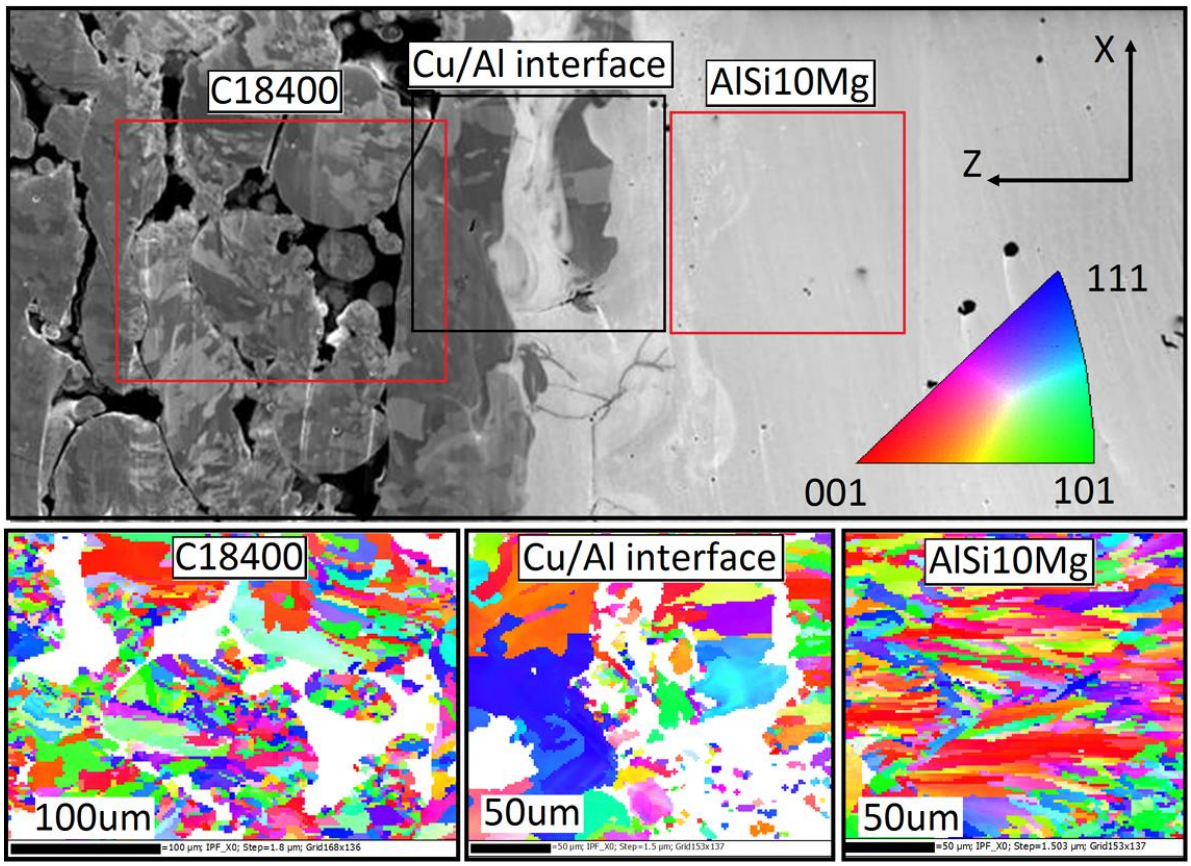

Fig. 5. EBSD results at the copper, Cu/Al interface and AlSi10Mg

At the C18400 copper area, a mixture of ultrafine equiaxed grains and elongated grains. The ultrafine grains formed are due to the higher cooling rates experienced during the SLM process as a result of higher thermal conductivity of copper. At the Cu/Al interface, larger equiaxed grains are obtained. The formation of larger grains can be due to the formation of intermetallic, resulting in lower thermal conductivity in the material. Elongated columnar grains are obtained in the AlSi10Mg region.

3.4 X-Ray Diffraction

The Al/Cu sample was carefully prepared and polished from the AlSi10Mg side, to the interface and finally to the C18400 side. XRD results from Fig. 6(a) coupled with SEM images observed from Fig. 2(d) of AlSi10Mg showed that it consisted mainly Al as the matrix and eutectic Si dendrites. From the FIB image shown in Fig. 2(c) and the XRD results from Fig.

6(b), it is shown that C18400 processed with SLM consist of equiaxed grains of copper. From the Cu-Al phase diagram, a wide range of Cu-Al phases can be formed, and based on the XRD results shown in Fig. 6(c) and Fig. 6(d), it is shown that the intermetallic Al_2Cu was formed from both the copper and aluminum sides. However, the formation of intermetallic phases cannot be exclusively explained using on the phase diagram [16].

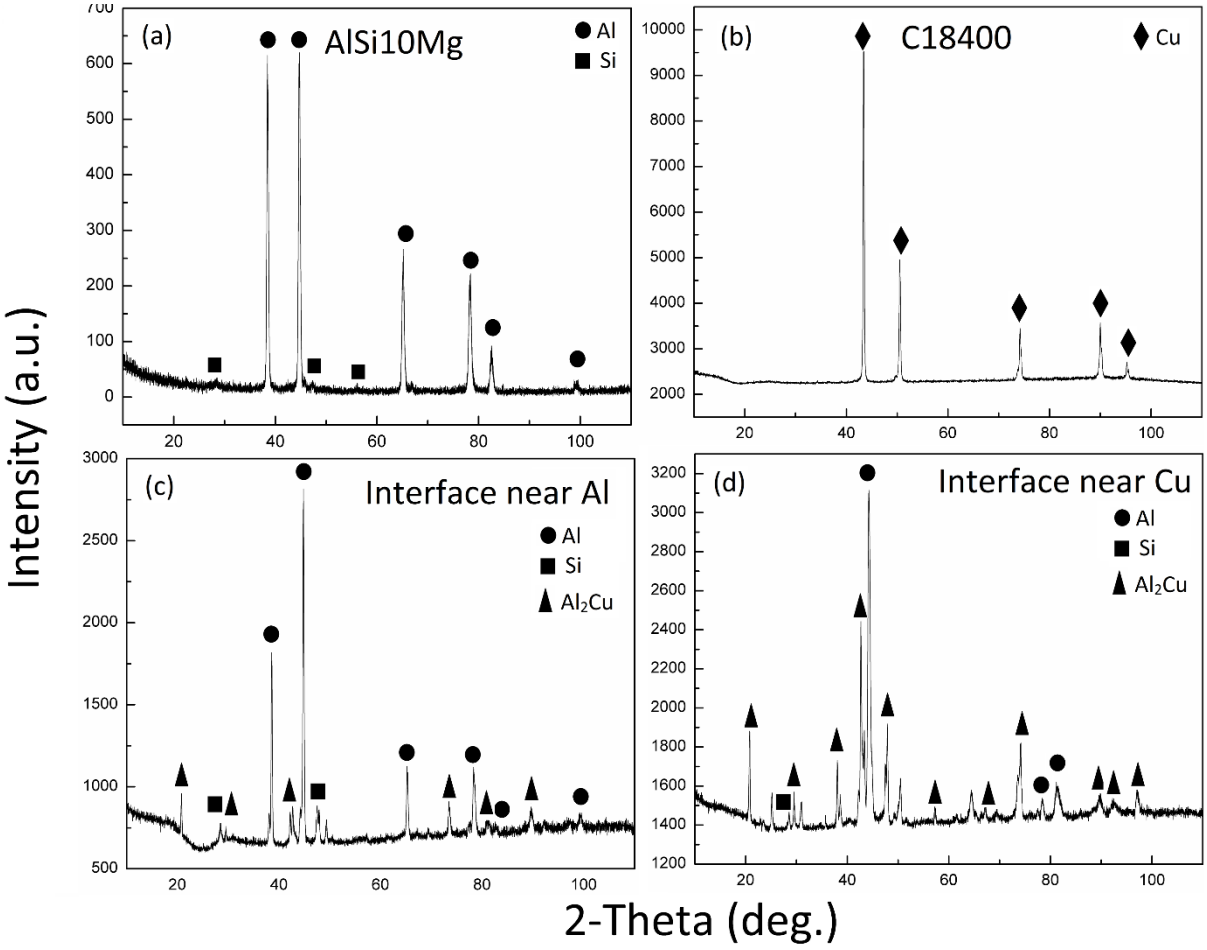

Fig. 6. XRD results. (a) AlSi10Mg; (b) UNS C18400; (c) Interface closer to Al; (d) Interface closer to Cu

During the SLM process, the high temperatures associated with the process and the formation of Al/Cu solid solution results in the formation of the intermetallic as there is incorporation of Al atoms in the Cu structures. From crystalllography point of view, Al_2Cu is formed preferably as there are less atoms in the crystal unit cell. Al_2Cu has 12 atoms per unit cell and a short

range order, compared to AlCu (20 atoms per unit cell) and Al_9Cu_4 (52 atoms per unit cell) [17]. Thus, it is reasonable to deduce that Al_2Cu nucleates first during the SLM prcoess. From the phase diagram, it is possible to observe the formation of this phase results from a peritectic reaction which occurs at 590 ^oC [18], and during SLM, the formation of this compound can be based on a thermomechanical induced solid state diffusion process. The variation of the copper, Al, Si and Al_2Cu peaks across the different regions corroborate the complex mixing of copper and AlSI10Mg in the interface. The binary phase diagram for copper and aluminum also shows on the copper side a region of solubility of aluminum, while on the aluminum side no solubility for copper in aluminum is present. The formation of intermetallic compounds can be controlled by restricting the dilution between the two materials and reduce their interaction time [8]. This can be done by reducing the laser power, increasing the scanning speed or hatch spacing so as to control the dimensions of the melt pools formed during SLM.

4. Al/Cu Mechanical Properties

4.1 Tensile Test

A sample of tensile coupons used in the tensile test are shown in Fig. 7.

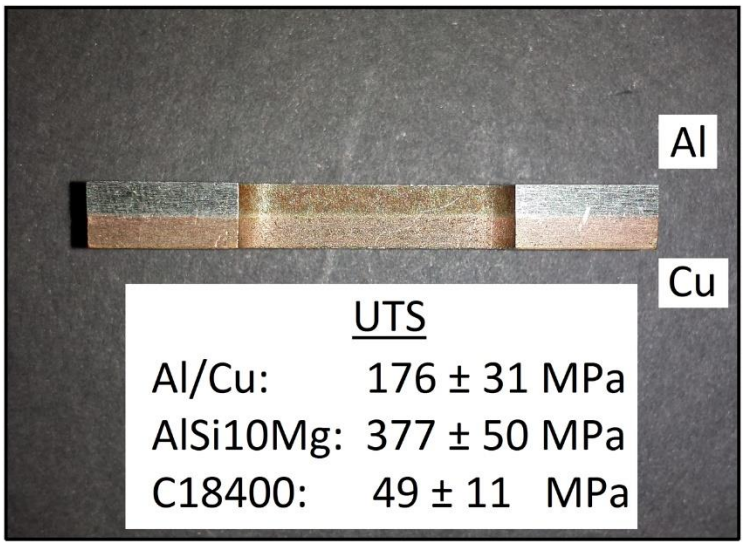

Fig. 7. Sample of tensile coupons for Al/Cu

The ultimate tensile strength (UTS) measured for Al/Cu, AlSi10Mg and C18400 is 176 ± 31 MPa, 377 ± 50 MPa and 49 ± 11 MPa respectively. The UTS measured shows that the failure occurs predominantly and firstly at the copper side. This means that the interfacial bond strength between aluminum and copper is stronger than the copper itself. The tensile tests results agree with the microstructural analysis of the interface which shows that the interface is denser than the copper region.

The fracture surface of Al/Cu parts after tensile test is shown in Fig. 8. A detailed observation of the tensile fracture of the Al/Cu part shows that the fracture is a mixture of ductile and brittle modes, where ductile mode is observed to be more prominent. At the copper region, numerous unmelted particles and several porous voids were observed. The fracture surface did not show any observable characteristics of a typical tensile fracture. This indicates inadequate bonding between each copper layer as a result of insufficient melting during SLM. At the aluminium region, smooth, flat ridges with high fracture planes and sharp edges were observed from the fracture surface. Furthermore, distinctive gradual ridges suggest tearing of metal and manifestation of plastic deformation corresponding to ductile fracture.

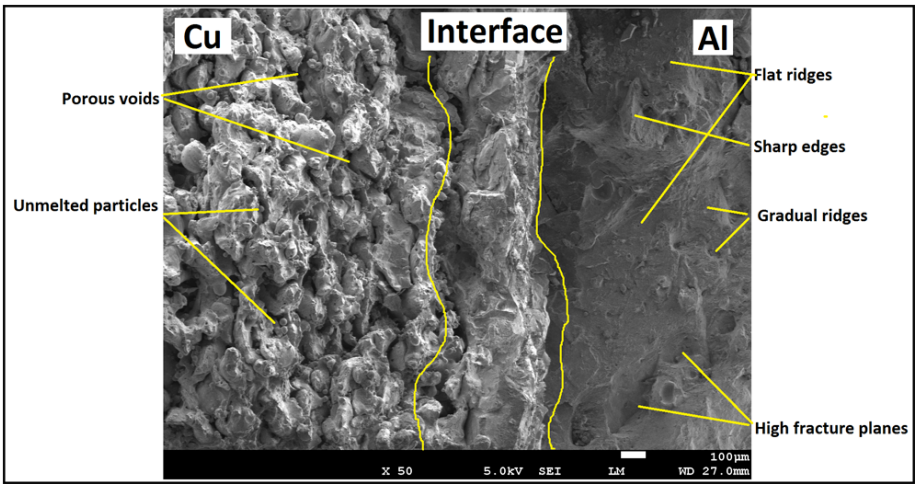

Fig. 8. Fracture characteristics of Al/Cu SLM part

4.2 Bending Test

A three point bending test was applied to the SLM samples, with Al and Cu at root respectively, to determine the strength of bonding between the two materials and the interfacial strength. The samples have width of 15 mm, thickness of 5 mm and the support span used is 40 mm. Load was applied until the samples fracture. Bending strength reflects resistance to bending deformation and is affected by bonding strength between the layers, surface layer strength and the thickness ratio between layers [19]. The fracture modes encountered in the three-point bending test were classified as: (1) adhesive: along the intermixed region between AlSi10Mg and C18400; (2) cohesive: entirely within AlSi10Mg or C18400; or (3) mixed: a mixture of adhesive fracture and cohesive fracture. The flexural stress-strain curves and the bended samples are shown in Fig. 9.

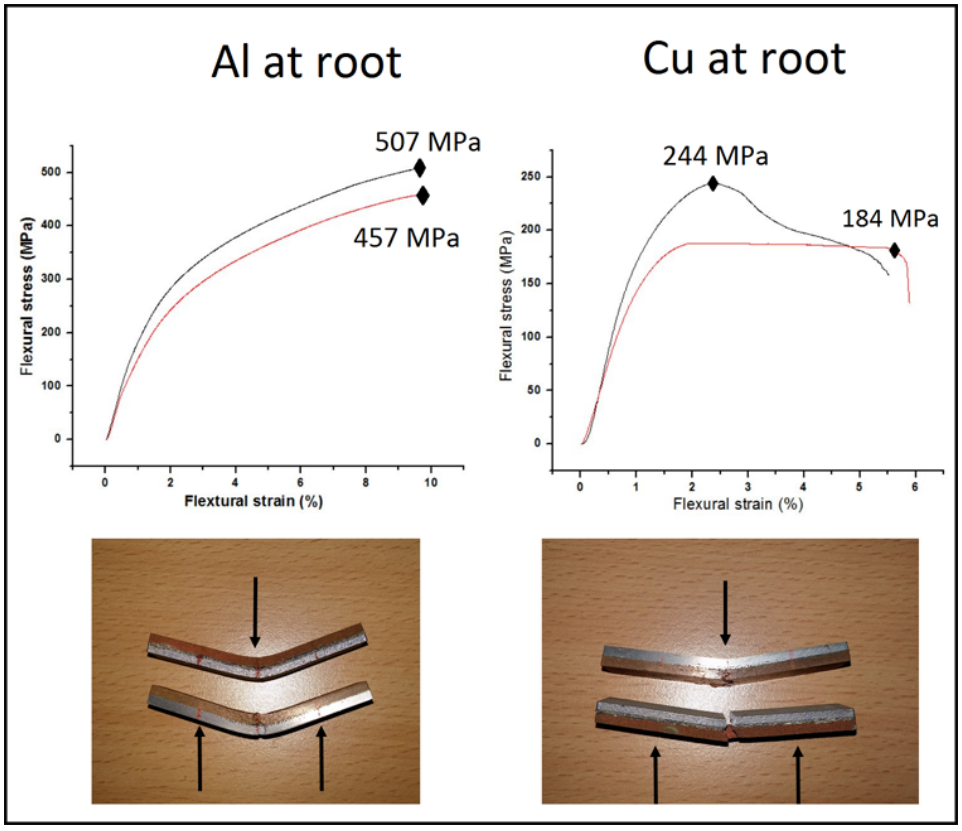

Fig. 9. Flexural stress-strain curves and bended samples

After bending up to flexural strain of 10 %, the samples were not separated, torn or cracked at the interface, indicating good metallurgical bonding between AlSi10Mg and C18400 and potential for the SLM samples to be deformed or shaped. Visual inspection of each tested specimen showed that all cracks occurred across both AlSI10Mg and C18400 which was mixed fracture. This also shows that the delamination resistance of the interface is higher than the ultimate flexural strengths of the individual materials. When Al is at the root during the bending test, the bimetallic Al/Cu strip is able to withstand the bending up to 10 % strain without any fracture, this can be attributed to the high strength of Al, maximum strengths of 457 MPa and 507 MPa are recorded. In contrast, when the Cu is at the root during the bending test, the Al/Cu strip fractured before strain of 10 % is reached. The Al/Cu strips fractured at 184 MPa and 244 MPa. This can be due to the higher porosity and the lower strength of the copper. This shows that the majority of the loading bearing is still done by Al in the strips. Furthermore, when Cu is at root, Al underwent compression while Cu underwent tension, resulting in premature fracture of the sample as compared to when Al is at root. The difference in loading conditions between the two sets of test also accounted for the higher strength for Al and Cu recorded when Al is at root, compared to when Cu is at root. This may be due to the porous nature of Cu, which results in increased sensitivity to tension failure, leading to crack propagation from Cu to the interface to Al at lower strain values during the test when Cu is at root.

From the results, they indicate that the bending properties of the SLM samples are affected by the loading conditions due to the dissimilar mechanical properties of the constituent materials. The bonding strength between the materials is also affected by the elemental diffusion between the materials, i.e. the properties of the intermixed regions discussed previously, which in turn, are affected by the SLM processing parameters. However, they are in good agreement with

applications that required the good thermal conductivity of copper enhanced by the higher strength of AlSi10Mg.

4.3 Microhardness

Vicker's hardness test was carried out to understand the variation on microhardness across the interfacial region. The microhardness was measured from the copper region to the aluminum region, with 6 indentations across each region. At the copper region, microhardness value was measured to be 71.74 ± 7.5 HV and at the aluminum region, the microhardness value was measured to be 119.06 ± 9.12 HV. Across the interface, the microhardness values are observed to increase gradually and almost linearly from the copper to aluminum region, however, anomalous microhardness values are also recorded in the interface. The variation of microhardness value across the interface is shown in Fig. 10.

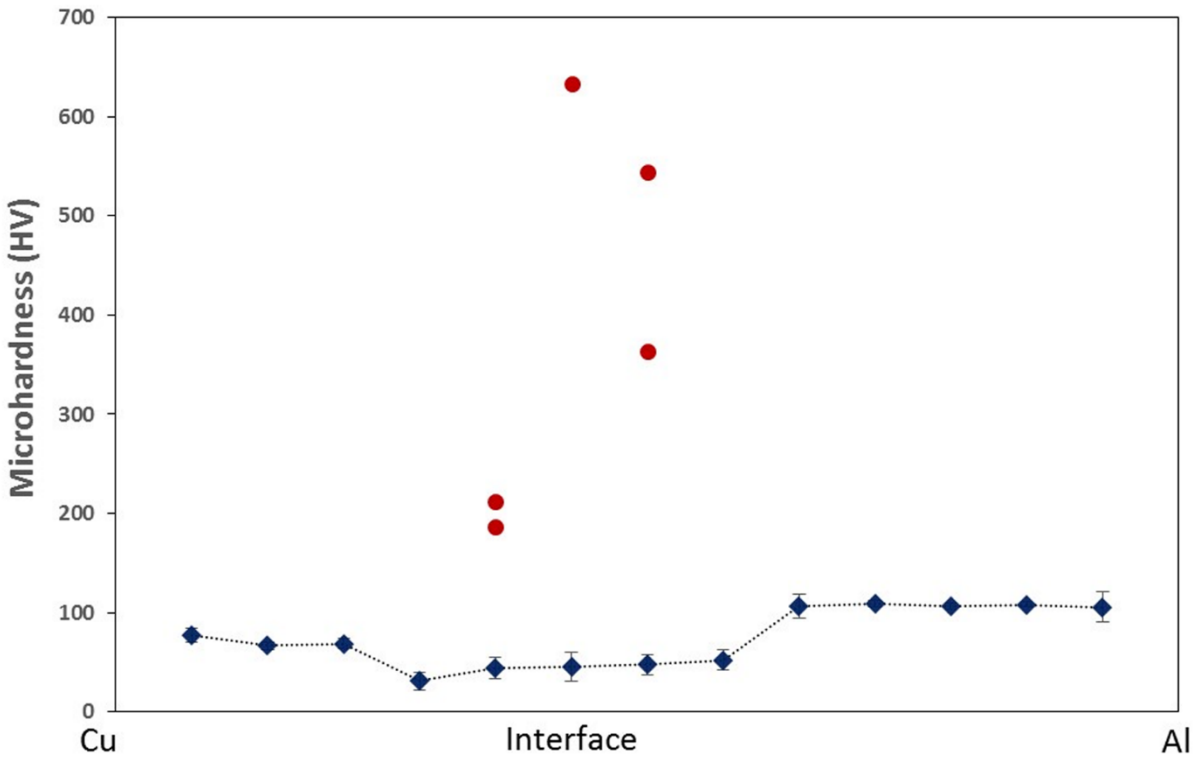

Fig. 10. Microhardness variation along the Al/Cu interface

The anomalous readings for micro-hardness recorded at the interface are due to formation of harder but more brittle intermetallic Al_2Cu which can have values of 400 to 600 HV [20]. The gradually increase in microhardness across the interface is due to dilution effect. Across the interface from copper to aluminum region, the proportion of copper decreases as more aluminum is melted in the melt pools formed. This leads to the gradual increase in microhardness.

5. Conclusion

In this work, multi-material processing of AlSi10Mg and UNS C18400 was successfully carried out by SLM. The interfacial characteristics of Al/Cu bimetallic laminates have been characterized and the key findings are:

1. Good metallurgical bonding was obtained at the interface between AlSi10Mg and C18400
2. An intermixed region was formed between the two materials and intermetallic compound Al_2Cu is formed in this region due the elemental diffusion during SLM
3. The bimetallic Al/Cu laminates exhibited higher tensile strength than that of copper but lesser than that of AlSi10Mg
4. Bending test results concluded the good bonding strength between AlSi10Mg and C18400 by SLM

Despite the potential of SLM for multi-material processing shown in this study, there are still some limitations that need to be overcome. One of the limitations is the heat treatment of the SLM formed multi-material parts. Different materials may require different heat treatment, thus, by having two or more materials in a formed and ready to use parts can complicate the post processing. However, specific heat treatments can be designed and customized for such parts in the future.

The separation of the mixed powders that are not irradiated by the laser, or collected in the overflows during the SLM process is another challenge in multi-material processing. The authors propose two methods for future work:

1. Use of magnetic material. One of the powder used can be magnetic while the other is not. In this way, the powder mixed can be separated by using magnets. For example, ferritic steel can be processed with non-magnetic materials such as aluminum.
2. Use of powders of different particle size distribution. The powders can then be separated using sieving in inert environment. For example, one of the powders used can have a maximum size of 20 μm and the other has a distribution of 25 μm to 65 μm. In this case, the powders can easily be separated by sieving after SLM.

REFERENCES

[1] C.K. Chua, K.F. Leong, 3D Printing and Additive Manufacturing: Principles and Applications, 4th ed., World Scientific Publishing Co. Pte. Ltd, Singapore, 2014.

[2] L.E. Loh, C.K. Chua, W.Y. Yeong, J. Song, M. Mapar, S.L. Sing, Z.H. Liu, D.Q. Zhang, Numerical investigation and an effective modelling on the Selective Laser Melting (SLM) process with aluminium alloy 6061, International Journal of Heat and Mass Transfer, 80 (2015) 288-300.

[3] S.L. Sing, W.Y. Yeong, C.K. Chua, F.E. Wiria, Z.H. Liu, D.Q. Zhang, B.Y. Tay, Classical Lamination Theory applied on parts produced by Selective Laser Melting, High Value Manufacturing: Advance Research in Virtual and Rapid Prototyping, (2013) 77-82.

[4] Z.H. Liu, D.Q. Zhang, S.L. Sing, C.K. Chua, L.E. Loh, Interfacial characterization of SLM parts in multi-material processing: Metallurgical diffusion between 316L stainless steel and C18400 copper alloy, Materials Characterization, 94 (2014) 116-125.

[5] C.A. Terrazas, S.M. Gaytan, E. Rodriguez, D. Espalin, L.E. Murr, F. Medina, R.B. Wicker, Multi-material metallic structure fabrication using electron beam melting, International Journal of Advanced Manufacturing Technology, 71 (2014) 33-45.

[6] V. Mohammad, S. Chianrabutra, B. Mellor, S. Yang, Multi material additive manufacturing - Part 1: a review, Virtual and Physical Prototyping, 8 (2013) 19-50.

[7] O.M. Al-Jamal, S. Hinduja, L. Li, Characteristics of the bond in Cu-H13 tool steel parts fabricated using SLM, CIRP Annals - Manufacturing Technology, 57 (2008) 239-242.

[8] J.P. Bergmann, F. Petzoldt, R. Schürer, S. Schneider, Solid-state welding of aluminum to copper - case studeis, Welding in the World, 57 (2013) 541-550.

[9] K.Y. Rhee, W.Y. Han, H.J. Park, S.S. Kim, Fabrication of aluminum/copper clad composite using hot hydrostatic extrusion process and its material characteristics, Materials Science and Engineering a-Structural Materials Properties Microstructure and Processing, 384 (2004) 70-76.

[10] X. Li, G. Zu, P. Wang, R. Xu, Effects of Asymmetrical Roll Bonding on Microstructure, Chemical Phases and Properties of Copper/Aluminum Clad Sheet, John Wiley & Sons, New Jersey, 2012.

[11] T.A. Mai, A.C. Spowage, Characterisation of dissimilar joints in laser welding of steel-kovar, copper-steel and copper-aluminium, Materials Science and Engineering: A, 374 (2004) 224-233.

[12] W.E. Veerkamp, Copper-to-aluminum transitions in high DC bus systems, Ieee Transactions on Industry Applications, 33 (1997) 1027-1034.

[13] D.Q. Zhang, Z.H. Liu, C.K. Chua, Investigation on forming process of copper alloys via Selective Laser Melting, High Value Manufacturing: Advance Research in Virtual and Rapid Prototyping, (2013) 285-289.

[14] Z.H. Liu, D.Q. Zhang, C.K. Chua, K.F. Leong, Crystal structure analysis of M2 high speed steel parts produced by selective laser melting, Materials Characterization, 84 (2013) 72-80.

[15] M.S. Anand, S.P. Murarka, R.P. Agarwala, Diffusion of Copper in Nickel and Aluminum, Journal of Applied Physics, 36 (1965) 3860-3861.

[16] I. Galvao, J.C. Oliveira, A. Loureiro, D.M. Rodrigues, Formation and distribution of brittle structures in friction stir welding of aluminium and copper: influence of process parameters, Science and Technology of Welding and Joining, 16 (2011) 681-689.

[17] H. Xu, C. Liu, V.V. Silberschmidt, Z. Chen, J. Wei, M. Sivakumar, Effect of bonding duration and substrate temperature in copper ball bonding on aluminium pads: A TEM study of interfacial evolution, Microelectronics Reliability, 51 (2011) 113-118.

[18] J. Ouyang, E. Yarrapareddy, R. Kovacevic, Microstructural evolution in the friction stir welded 6061 aluminum alloy (T6-temper condition) to copper, Journal of Materials Processing Technology, 172 (2006) 110-122.

[19] N. Masahashi, K. Komatsu, S. Watanabe, S. Hanada, Microstructure and properties of iron aluminu alloy/CrMo steel composite prepared by clad rolling, Journal of Alloys and Compounds, 379 (2004) 272-279.

[20] L. Dubourg, H. Pelletier, D. Vaissiere, F. Hlawka, A. Cornet, Mechanical characterisation of laser surface alloyed aluminium-copper systems, Wear, 253 (2002) 1077-1085.